Super Resolution Reconstruction in Mixed Noise Environment

A.Geetha Devi
Dept.,of ECE
PVP Siddhartha Inst. of Tech.,
Kanuru,Vijayawada, India.

T.Madhu
Swarnandra Institute of Engg.& Technology.,
Narasapuram, India.

K.Lal Kishore
Jawaharlal Nehru Technological University,
Ananthapur, India

ABSTRACT
A hybrid Super Resolution (SR) algorithm is proposed to deal with the Low Resolution (LR) images degraded by Mixed (Gaussian + Impulse) noise. The algorithm adaptively estimates and removes the impulse noise from the input LR images based on edge, geometrical & size characteristics. The fuzzy based impulse noise removal algorithm is along with adaptive sharpening filter based SR using steering kernel regression are used to obtain a HR image. The experimental results confirm the efficacy of the algorithm for different types of images at various noise densities.

General Terms
Super Resolution, Mixed Noise, Surveillance applications,

Keywords
Geometric features, Steering kernel regression, SIFT based registration, Interpolation.

1. INTRODUCTION
Image processing applications like surveillance systems, forensic sciences, medical imaging, pattern recognition, remote sensing, video transmission, High Definition Tele Vision (HDTV) and web applications require images at High Resolution (HR) for their efficient quality and functioning. The resolution of the image depends on the image acquisition system. The improper lens adjustment of the camera and the focal distance will also limit the resolution of the acquired images. The images are further degraded by the noise due to external environment and the blur introduced through the moment of the camera or object. The camera manufacturing technology could not meet the requirement due to the cost efficiency and other practical limitations like shot noise. These limitations gave rise to the development of signal processing based techniques to apply on the acquired LR images called the Super Resolution (SR) Image Reconstruction Techniques. SR Reconstruction is a procedure of attaining High Resolution (HR) image from a set of Low Resolution (LR) observations [1].

A single image SR requires a large database to reconstruct the image. Multi image Super resolution algorithms include the stages of image registration, Image fusion, Image interpolation and restoration. The multiple images with sub pixel shifts are registered to align the LR images onto a common geometrical plane [2]. The accuracy of the registration method will decide the efficiency of the SR algorithm. The registered LR images are applied to fusion algorithm to integrate the sub pixel information in them [3]. The fused image is then interpolated to improve its resolution and is applied to restoration process for the removal of blur and noise.

In real time applications, the acquired image quality is predominantly affected by noise sources, internal as well as external. Usually the additive noise component in LR images is modeled as additive white Gaussian noise, but when the image is transmitted through a communication channel, image transmission noise, atmospheric disturbances and imperfections in transmission lines will contribute to impulsive noise. Thus, noise corruption process in simulated scenarios is modeled using additive Gaussian noise, impulsive noise, or mixed noise. Further, the continuous improvement in the optical resolution will result in the improvement of noise levels and graininess in the original image due to the increased sensitivity to noise and hence the reduced Signal to Noise Ratio (SNR). The denoising process of images requires accurate noise estimation i.e., if the estimation is too low, noise will be large and if the estimation is too high then many image details are erased from the image. There are many noise removing filters available in literature for Gaussian noise, impulse noise as well as for mixed noise environment [4]. The selection of the restoration process should not affect the other stages of SR reconstruction. Hence, an optimum solution is required to estimate and remove the noise from images while improving the resolution.

In order to deal with SR reconstruction in mixed noise environment, the proposed algorithm employs a fuzzy based adaptive impulse noise estimation and removal algorithm followed by Adaptive sharpening filter based SR algorithm [5]. In this paper Section 2 describes the problem formulation and observation model. Section 3 explores the proposed algorithm and Results & discussion are depicted in Section 4. The concluding remarks are explained in Section 5.

2. PROBLEM FORMULATION
The process of image formation includes degradations like image translation or rotation, blur and additive noise. Due to the optical distortions like out of focus or diffraction limit, there will be a natural loss of spatial resolution. Limited shutter speed of the camera and noise cause blur and insufficient sensor density will cause aliasing [2]. Hence to reconstruct a HR image an observation model is formulated that relates the HR and LR images as shown in Fig.1.

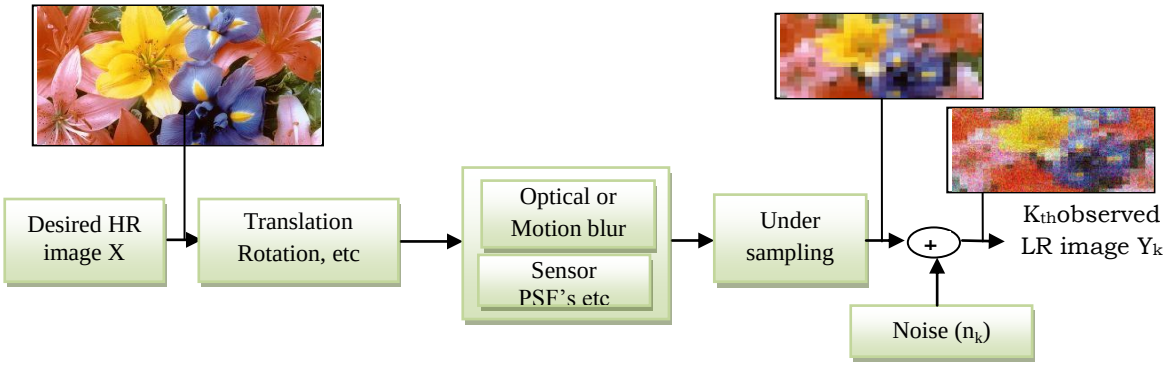

Fig: 1. Camera Observation model relating LR and HR images

Consider the HR image X and the low resolution images as $Y_{k.}$ Where k=1……..p and p is the value of number of low resolution images. From the observation model [2], the LR image can be represented as

$$Y_{c,k} = DB_kM_kX_c + N_{c,k} \quad \text{for color images} \qquad \ldots(1)$$

Here D is the down sampling matrix, B_k is the blur, M_k is the warping matrix and N_k is the additive mixed noise. Xc is the c^{th} color component of unknown High resolution image, $y_{c,k}$ is the k^{th} Low resolution image of the Xc. Super Resolution will become an ill posed inverse problem as the HR image X is obtained by applying the inverse of all the degradation functions on a set of low resolution images and in this process if the degradation function kills any of the high frequency components, then the solution to get the HR image will not be unique [1].

In multiple SR reconstruction algorithms, Registration stage is used to compensate for the of various displacements that occur during image acquisition process like moving and tilting camera or the object. [6].Image Fusion is to combine the new information existing in the LR images due to their sub pixel shifts [3]. Interpolation is to compensate the effect of down sampling of original object due to the distance from the camera, insufficient sensor density and lens adjustments during image acquisition [2]. Restoration is used to recover the original image from the blurred and noisy images [7]. All these stages are applied sequentially or simultaneously depending on the required applications.

3. PROPOSED ALGORITHM

In the developed multi SR algorithm mixed noise (a combination of both impulse and Gaussian) is considered. [4], [8]. The impulse noise elimination is achieved through the Adaptive Geometric Feature based Filter (AGFF) restoration algorithm [9] and all the LR images have to undergo this process prior to registration. In high noisy conditions the AGFF based restoration algorithm may introduce blur into the system. Hence to preserve the edge information and to remove the zero mean Gaussian random noise, the SR algorithm using adaptive sharpening filter based on kernel regression is utilized. The algorithm is also well suited for removing the color artifacts.

In this proposed algorithm, Feature based registration using SIFT algorithm is applied for registration [10-12]. The registered images are fused by the Singular Value Decomposition (SVD) based fusion [13] which is an optimal fusion algorithm. The resolution of the fused image is improved by the Bi-cubic interpolation algorithm [14] and adaptive sharpening filter restoration [15] is employed for the removal of Gaussian noise and blur component if any. The proposed algorithm is illustrated in the Fig.2.

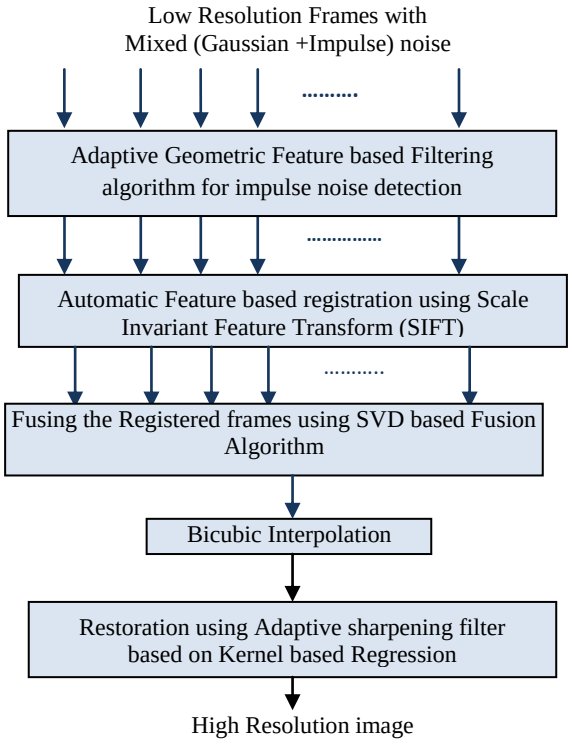

Fig: 2. Proposed SR Algorithm in mixed noise environment

3.1 Adaptive Geometric Feature based Filtering (AGFF) algorithm

The impulse noise is two types: salt & pepper noise and random impulse noise. The uncorrupted portions of the colour image always exhibit a certain degree of smoothness, where as the corrupted noise regions will be represented either by an isolated point, a short line, a cross of two short thin lines or other small round shaped blocks as shown in the Fig.3. The intensity values of the corrupted pixels always change gradually in all its 8-neighbour directions or in at least one direction [16].

The criteria for identifying the edge feature around the pixel is based on two types of derivatives G^a & G^d, which are approximated by pixel differences in digital colour images. For a vector color component $x(c) = [x_R(c),x_G(c),x_B(c)]^T$ of the colour image, the derivative G^a *is* $\eth x(c)/\eth c^a$ at c=*(i,j) and* is

evaluated by taking the difference between the pixel and its 4-neighbors for each component of the color pixel.

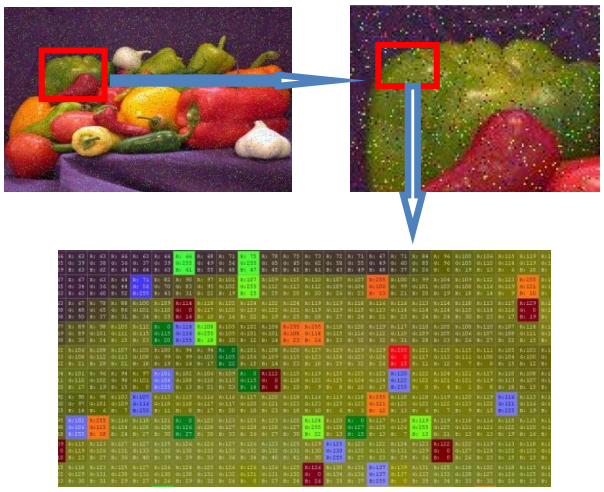

Fig.3: Geometrical Features of Impulsive Noise

The following equations are used for finding four neighbours of the central pixel [9]

$$G_1^a(n_1^a)=x[i,j]-x[i-n_1^a,j] \quad \ldots(2)$$

$$G_2^a(n_2^a) = x[i,j] - x[i,j-n_2^a] \quad \ldots(3)$$

$$G_3^a(n_3^a) = x[i,j] - x[i+n_3^a,j] \quad \ldots(4)$$

$$G_4^a(n_4^a) = x[i,j] - x[i,j+n_4^a] \quad \ldots(5)$$

Where $n^a=[n_1^a, n_2^a, n_3^a, n_4^a]^T$, $n_k^a>0$ Default value of n_k^a is 1 for $1\le k\le 4$.

When the derivative alone is considered in the diagonal direction, $\partial x(c)/\partial c^d = G^d$, the difference between the pixel and its 8-neighbors, for each component of the colour pixel [104] are given by

$$G_1^d(n_1^d) = x[i,j] - x[i-n_1^d,j-n_1^d] \quad \ldots(6)$$

$$G_2^d(n_2^d) = x[i,j] - x[i+n_2^d,j-n_2^d] \quad \ldots(7)$$

$$G_3^d(n_3^d) = x[i,j] - x[i+n_3^d,j+n_3^d] \quad \ldots(8)$$

$$G_4^d(n_4^d) = x[i,j] - x[i-n_4^d,j+n_4^d] \quad \ldots(9)$$

Where $n^d=[n_1^d, n_2^d, n_3^d, n_4^d]^T$, $n_k^d>0$ Default value is 1 for $1\le k\le 4$. The two special derivatives, G^a and G^d, will be used to measure the edge feature and other geometric properties to determine whether the center pixel at $c=(i,j)$ is corrupted or not.In detecting and removing impulse noise, a filter may make three main types of mistakes. Type I error (miss) occurs when there is a corrupted pixel which the filter does not detect. Type II error (false alarm) occurs when the filter detects an impulse noise pixel which is actually clean. When the filter removes an impulse noise and replaces it with a value determined by a certain restoration strategy, Type III error (over- or under-corrupting error) is defined as the difference between the resultant value after the restoration process and the true pixel value as the noise-free pixel was.

3.2 Adaptive Geometric Feature based Filtering (AGFF) method

AGFF technique is a novel impulse detection scheme based on the 2-D geometric information of the corrupted pixels. The corrupted pixels are classified into four sets S1, S2, S3 & S4.

Set S_1 includes individual impulse pixels, slant noise lines with one-pixel width and the pixels of the lines adjacent to each other only in diagonal direction within the defined length. In terms of the pixel coordinates of a colour image, C, a set of corrupted pixels is defined as

$$S_1 = \{c \mid ((G^a < (-T_e)) \,\&\, (G^d < (-T_e)>))) \; V \; ((G^a > T_e) \,\&\, (G^d > T_e))$$
$$\text{when } n_k^a = 1 \text{ for } 1\le k\le 4,\ n_k^d = \{1,2,3,\ldots T_m\},$$
$$T_m = (T_l+1)/2\} \quad \ldots(10)$$

where T_e is the edge-feature-identification threshold that represents the value of a derivative to distinguish the sharp step edges from other types of edges, T_l is the length threshold and may be defined according to the noise ratio and T_m is used to define corrupted pixel-sizes in S_1 and has a default value of 2.

A set of corrupted pixels, which include individual impulse pixels, straight noise lines with one-pixel width and the pixels of the lines being only 4-neighbors to each other with the defined length of T_l, is defined as set S2 and is given by

$$S_2 = \{c \mid ((G^a < (-T_e)) \,\&\, (G^d < (-T_e)>))) \; V \; ((G^a > T_e) \,\&\, (G^d > T_e))$$
$$n_k^d = 1 \text{ for } 1\le k\le 4,\ n_k^a = \{1,2,3,\ldots T_m\},\ T_m = (T_l+1)/2\} \quad \ldots(11)$$

Where T_m is used to define the corrupted pixel-sizes in this set and has a default value of 2.

Next, a set of corrupted pixels that include noisy pixels/regions within 3-pixel width in any direction except the noisy pixels already present in S1 and S2 i.e.,

$$S_3 = S - (S_1 U\, S_2) \quad \ldots(12)$$

where $S=\{c \mid ((G^a<(-T_e)) \,\&\, (G^d<(-T_e)))) \; V \; ((G^a>T_e) \,\&\, (G^d>T_e))$
and $n_k^a = n_k^d = L,\ L=2 \text{ or } 3,\ 1\le k\le 4.$ ...(13)

The two partial derivatives G^a & G^d have magnitudes greater than the preset threshold T_e.

Finally, according to observations and analysis of a variety of natural images corrupted by the impulse noise, a protrusive point in the border area with high possibility of being a corrupted pixel is defined as

$$S_4 = \{c \mid ((G_k^a < (-T_e)) \,\&\, (Gv^d < (-T_e)))) \; V \; ((G_k^a > T_e) \,\&\, (G_v^d > T_e))$$
$$n_k^a = n_k^d = n_v^a = n_v^d = 1. \quad \ldots(14)$$
$$\forall k = \{y/(y \in N_n \wedge y \neq e)\}, e \in N_n, N_n = \{1,2,3,4\}$$
$$(v = k) \wedge (v \in \{2,3\}) \vee (v \in \{3,4\}) \vee (v \in \{4,1\})(v \in \{1,2\})$$

If the two partial derivatives G^a and G^d of a pixel have the same sign while their magnitudes are greater than the preset threshold T_e, with the partial derivatives indexed by k containing only three out of the four distance settings, and the partial derivatives indexed by v being either {2, 3} or {3, 4} of {4, 1} or {1, 2} and equal to k. Then the pixel belongs to S_4.

The proposed definitions of the corrupted pixel sets in color images are tested by experiments using typical test image including real-life images [9]. The shape and size of the corrupted pixels depend on the noise ratio, and the restoration of the corrupted pixels requires statistical information about the noise density.

3.2.1 AGFF Implementation

Impulse noise reduction can be possible by the application of median filter but it may cause artifacts to the uncorrupted pixels. Hence, to avoid the drawbacks a detection scheme is utilized before applying median filter. As a result, the

proposed restoration method based on the restricted median can keep the image unchanged when the filter processing window moves across the uncorrupted image details. It is expensive to perform a sort on pixels within a large rectangular window. If the width of processing window is larger than three, a modified median filter [16] can be applied alternatively in the AGFF technique. Restoration using median filter may cause destruction of noise-free pixels i.e., Type II error becomes increasingly severe with an increase in the processing window size while it is less likely with the increase of the edge feature threshold Te. Hence, the design of the processing windows has to depend on the shape and size of corrupted pixels/pixel regions in order to achieve the best performance, in terms of both visual quality and objective measurements.

At each coordinate c € C, a square filter processing window centers at the coordinate c and contains N pixels, where N is an odd number. The width of the window is represented as √N and must be a positive integer, i.e., 3, 5, 7, and so on, in the recommended implementation. The operations for removing impulses in S_1, S_2, and S_4 are implemented by a 3X3 processing window, and the operation to remove impulses in S_3 is implemented by a 5X5 processing window. Each processed pixel in colour image is at the centre of the symmetric window.

The threshold to discriminate the corrupted pixel and its neighborhood is usually set to less than 20 in magnitude for the filter, in order to improve perceptual image quality (i.e., reducing Type I error). However with the decrease of threshold Te, the filter removes more and more uncorrupted details of the image during its operation. It is important to see that the Type II error is also under good control in order to preserve the uncorrupted details, structures, and features of the image as much as possible. A balance between noise removing and preservation of the details must be made based on the optimization of objective measurements. In the following implementation, the threshold T_e is chosen from a range adaptive to the size of the processing window. The value of T_e is set at 15 for detecting the pixels in S1 and S2, 40 for S3 and 35 for S4 pixels.

3.2.2 Image Noise Estimation

Estimation of impulse noise ratio and the type of corrupted image are obtained by analysing the ratio and values of S1 or S2 detected from the image, through a fuzzy rule based approach. The estimation results by S1 or S2 are similar to each other and, therefore as an example, the estimation by S2 is described as follows. A set of membership functions are given for noise free (μ_{free}), low noise ratio (μ_{low}), medium noise ratio (μ_{medium}), high noise ratio (μ_{high}) and very high noise ratio ($\mu_{very\text{-}high}$) of the fuzzy set.

$$
\begin{aligned}
\mu_{free} &= 1, && R_{s2}<0.0001\\
&= (0.002-R_{s2})/0.0019, && 0.0001\le R_{S2}\le 0.002\\
\mu_{low} &= (R_{s2}-0.0001)/0.0019, && 0.0001\le R_{s2}<0.002\\
&= 1, && 0.002\le R_{s2}<0.006\\
&= (0.02-R_{s2})/0.006, && 0.006\le R_{s2}\le 0.012\\
\mu_{medium} &= (R_{s2}-0.006)/0.006, && 0.006\le R_{s2}<0.012\\
&= 1, && 0.012\le R_{s2}<0.042\\
&= (0.048-R_{s2})/0.006, && 0.042\le R_{s2}\le 0.048\\
\mu_{high} &= (R_{s2}-0.042)/0.006, && 0.042\le R_{s2}<0.048\\
&= 1, && 0.048\le R_{s2}<0.074\\
&= (0.08-R_{s2})/0.004, && 0.074\le R_{s2}\le 0.08\\
\mu_{veryhigh} &= (R_{s2}-0.074)/0.004, && 0.074\le R_{s2}<0.08\\
&= 1, && R_{s2}\ge 0.08
\end{aligned}
\qquad ...(15)
$$

Where Rs_2 is the ratio of S_2 (except S1 ⋂ S2) detected from RGB channels of the image to the image size, i.e., Rs2= (the number of pixels in S2 (expect S1 ⋂ S2))/ the total num of pixels of the tested image.

The number of fuzzy membership functions associated with each variable depend on the denoising operations and the sum of fuzzy membership values where functions overlap is recommended to be one or less than one because the AGFF can tolerate the estimation deviation of the noise ratio. A simple trapezoidal shape is used as a function in the fuzzification process and the maximum method is used in defuzzification.

The design principle of operations, which are adapted to different noise ratios and types [17-20], is to use the size of the window as small as possible and as less number of the passes as possible, as long as the impulse noise can be removed. The number of pass is determined for removal of a noise region based on the worst case scenario within the estimated maximal size of the noise region. The operations designed for removing impulses from different corrupted pixel sets in natural digital color images, are to be applied on R, G, B channels separately. The flow chart of the restoration algorithm is depicted in Fig.4.

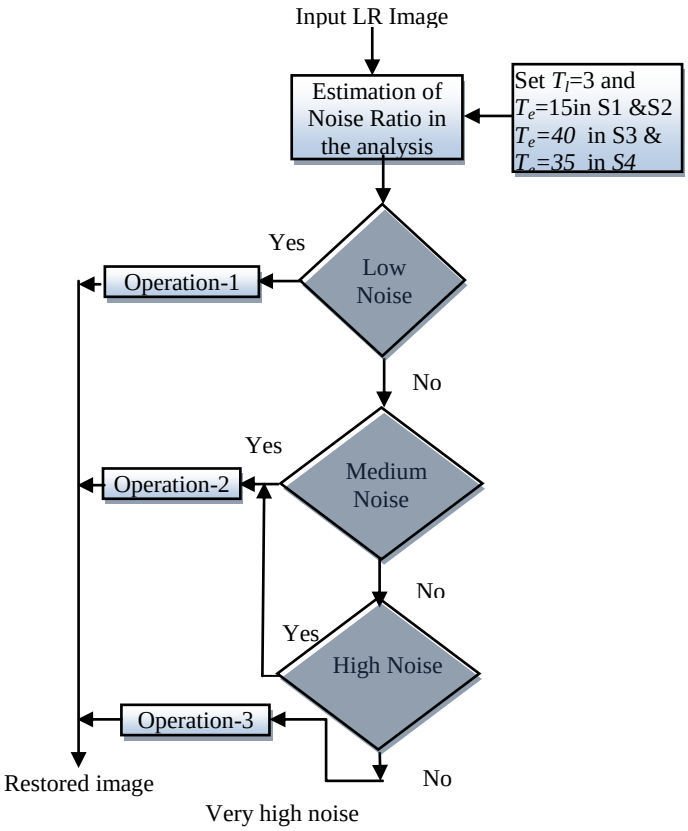

Fig. 4: Impulse Noise Restoration based on AGFF technique

Operation-1 consists of a median filtering operation to restore the colour images with a low noise ratio. In the first pass, it restores the impulse corrupted pixels in S1& S2.

Operation-2 consists of two pass median filtering. Operation 2 is designed to restore colour images with medium or high noise ratio.

Operation-3 Consists of operation 2, edge preserving operator and one-pass median filtering to restore pixels in S3. It is designed to restore the images with very high noise ratio.

Excellent convergence is observed by using the AGFF. Two passes of the operations may lead to a zero response for further repetition. That means, as an alternative, the operations in the above algorithm can be applied iteratively until reaching the stop criterion of zero response, without causing too many artifacts to the images. This property of operation is very useful to ensure perceptual quality and at the same time to minimize the risk of causing type 2 errors. Although the filter implemented by the above algorithm deals with noise ratio within 50% using the noise model defined to ensure good perceptual image quality, a large processing window size can be considered with the increase of noise ratio in color images, in order to remove all impulse noise which can be detected by the human eyes. However, this may result in destruction of finer image details, in terms of objective image quality measurements.

3.3 Automatic feature based registration using SIFT

Registration is the process of bringing all the shifted versions of low resolution images into a single plane with respect to a reference image. Feature based registration comprises of feature detection, feature matching, optimum transformation and up-sampling and provides better results in many applications. Automatic Feature based registration using Scale Invariant Feature Transform [10-12] is used for registration. These algorithms extract the distinct features from different images and are called as control points. The location and scale of these control points are determined by Scale Invariant Feature Transform (SIFT). The detection of location of the control points (SIFT keys) should be invariant to scale change, translation or rotation, since these keys can be repeatedly assigned to different views of the same object. The detection of the SIFT key locations is accomplished by searching for stable features across all possible scales, using a continuous function of scale known as scale space and can be determined only by Gaussian function [10]. These SIFT keys are obtained by using the Difference of Gaussian (DoG) filter [12].

Hence, the scale space of an image is defined as a function $M(x,y,\sigma)$, which is produced by convolving a variable scale Gaussian function $G(x,y,\sigma)$ with the input image $I(x,y)$.

$$M(x,y,\sigma) = G(x,y,\sigma) * I(x,y) \quad ...(16)$$

Where * is the convolution operator, x,y are the coordinators and σ is standard deviation of Gaussian Function defined by

$$G(x,y,\sigma) = \frac{1}{2\pi\sigma^2} e^{-(x^2+y^2)/2\sigma^2} \quad ...(17)$$

To detect the key points effectively in scale space, the Difference of Gaussian function is used to convolve the input image. The DoG function DoG(x,y,σ) is computed by taking the difference of two Gaussian functions with different standard deviations, separated by a constant multiplicative factor *k*. i. e.

$$DoG(x,y,\sigma) = \big(G(x,y,k\sigma) - G(x,y,\sigma)\big) * I(x,y)$$
$$= M(x,y,k\sigma) - M(x,y,\sigma) \quad ...(18)$$

The normalized Laplacian of Gaussian (LoG) operator, $\sigma^2\nabla^2 G$ [7], which has close approaximation to the DoG is required for the scale invariance. It is found that the maxima and minima of $\sigma^2\nabla^2 G$ will produce the most stable image features. The relationship between the DoG function and Laplacian function $\sigma^2\nabla^2 G$ can be understood from the heat diffusion equation.

$$\frac{\partial G}{\partial \sigma} = \sigma\nabla^2 G$$

$$\sigma\nabla^2 G = \frac{\partial G}{\partial \sigma} = \frac{\big(G(x,y,k\sigma) - G(x,y,\sigma)\big)}{k\sigma - \sigma}$$

$$G(x,y,k\sigma) - G(x,y,\sigma) \approx (k-1)\sigma^2\nabla^2 G \quad ...(19)$$

The DoG function has scales differing by a constant factor (k-1) over all scales and therefore does not influence extreme location. The approximation error goes to zero if k=1 but the approximation has no impact on the extreme detection or localization in practice. The maxima and minima are obtained by computing the pixel to its 26 neighbours in 3x3 regions at the current and adjacent scales. Maxima and Minima are selected only if it is larger than all of these neighbours or smaller than all of them. Most of the sample points will be eliminated in the first few checks. Hence the cost is reasonably low [10].Based on each gradient direction of each key point, the location will be given in one or more orientations. After assigning a consistent orientation to each key point based on the image local properties, the key point descriptor can be represented relative to this orientation and therefore achieve invariance to image rotation.

Towards a more stable local orientation, the scale of the key point is used to select the Gaussian smoothed image with the closest scale, so that all computations are performed in a scale invariant manner. For each image sample $M(x,y)$ at this scale, the gradient magnitude m(x,y) and orientation $\Theta(x,y)$ are pre computed using pixel differences [11].

$$m(x,y) = \sqrt{\big(M(x+1,y) - M(x-1,y)\big)^2 + \big(M(x,y+1) - M(x,y-1)\big)^2}$$

$$\theta(x,y) = \tan^{-1}\frac{M(x,y+1) - M(x,y-1)}{M(x+1,y) - M(x-1,y)} \quad ...(20)$$

An orientation histogram is formed from the gradient directions of sample points with in a region around the key point. The orientation histogram has 36 bins covering 360 degrees. Each sample added to the histogram is weighted by its gradient magnitude and by a Gaussian weighted circular window with a σ that is 1.5 times that of scale of the key point. The peaks in the orientation histogram correspond to the dominant directions of local gradients. First the highest peak in the histogram is detected and then any other local peak value that is within 80% of the highest value is used to create a key point with that same orientation. Therefore, for locations with multiple peaks of similar magnitude, there will be multiple key points created at the same location and scale but with different orientations. Although, only around 15% of the points are assigned multiple orientations, they will significantly contribute to the stability of matching. Finally a parabola is fit to the three histogram values closest to each peak value to interpolate the peak position for better accuracy.

Feature matching establishes the correspondence between the detected features of an image. The regular approach is to build local descriptors around the feature point and then match them. Euclidian distance matching, invariant moment and nearest neighbour based matching are the usual methods of feature matching [10].

RANdom SAmpling Consensus (RANSAC) [13], a strong feature estimator, classifies the matching features into inliers and outliers, where inliers are the features that hold on the model while the outliers will not. The RANSAC algorithm starts by randomly selecting the set of corresponding points. For each possible set of four key points in the reference image and the corresponding match in the target image, a mapping transform is found. The transformation matrix is estimated using

$$\begin{bmatrix} x' \\ y' \\ 1 \end{bmatrix} = T \begin{bmatrix} x \\ y \\ 1 \end{bmatrix} \quad ...(21)$$

Where $(x, y) \leftrightarrow (x', y')$ are the coordinates of the matching points in the target image and reference image respectively and T is the transformation matrix. The symmetric transfer error $d\,[(x,y), T(x', y')]^2 + d\,[(x', y'), T(x,y)]^2$ is calculated for every matching point and the inliers that are less than the threshold are counted. Here $d[(x,y), T(x', y')]$ is the Euclidian distance between pixel points with coordinates (x, y) and (x', y'). The same procedure is applied to the rest of key points in the reference image and the spatial coordinates of transformed key points are compared with the coordinates of the respective key points in the target image. The optimal model is one that supports the maximum number of key point pairs within the transform model.

3.4 Singular Value Decomposition (SVD) based fusion

The Singular Value Decomposition (SVD) technique is mainly utilized in facial feature extraction and recognition and is used in many SR reconstruction problems for effective identification of features in LR images [13]. The SVD of any image of size mxn is represented by

$$I = USV^T \quad ...(22)$$

where *U* and *V* are orthogonal to each other. The columns of *U* are eigen values of $I*I^T$ and the columns of *V* matrix are Eigen values of I^T*I. *U* is called left singular vector matrix and *V* is called right singular vector matrix. The diagonal elements of the *nxn* matrix *S* represent the intensity information of *I* and is called singular value matrix. The grey scale representation of any image is a two dimensional matrix and can be decomposed into SVD.

The highest singular value has the greatest amount of input information and the highest SVD lies at the upper left corner of the S matrix. Hence, let us represent the two input images I_1 and I_2 in the form of SVD as

$$I_1 = V_1 S_1 V_1^T \text{ and } I_2 = V_2 S_2 V_2^T \quad ...(23)$$

For the colour images, decomposition is performed in each color plane separately. Let the maximum values of S_1 and S_2 are β_{1max} and β_{2max} respectively. If $\beta_{1max} > \beta_{2max}$ then S_1 is used in the reconstruction of the fused image otherwise S_2 is used.

$$I_{fused} = V_2 S_{max} V_2^T \quad ...(24)$$

Where $S_{max}=S_1$ if $\beta_{1max} > \beta_{2max}$ &

$S_{max}=S_2$ if $\beta_{2max} > \beta_{1max}$

3.5 Bicubic Interpolation

In image processing, when speed is not an issue bi-cubic interpolation is often preferred over the nearest neighbourhood or bilinear interpolation [14]. Bi-cubic Interpolation is an application of cubic interpolation on 2-D and attempts to reconstruct the exact surface by extracting the sixteen pixels of image information from the closest 4x4 neighbourhood as shown in the Fig.5.

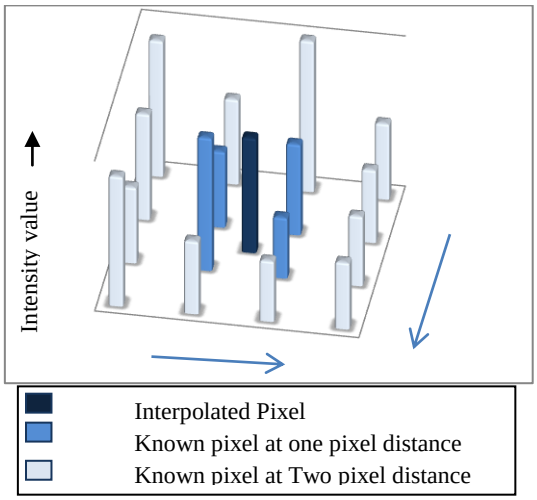

Fig.5: Pictorial representation of Bicubic interpolation

The bi-cubic interpolation kernel is

$$f(x) = \begin{cases} (a+2)|x|^3 - (a+3)|x|^2 + 1 & \rightarrow 0 < |x| < 1 \\ (a)|x|^3 - 5a|x|^2 + 8a|x| - 4a & \rightarrow 1 < |x| < 2 \\ 0 & \rightarrow elsewhere \end{cases} \quad ...(25)$$

Here, the closer pixels are assigned a higher weighting in the calculation. Bi-cubic produces noticeably sharper images than the previous two methods with negligible artifacts and is perhaps the ideal combination of processing time and output quality. For this reason it is a standard in many image editing programs, printer drivers and in-camera interpolation [21].

3.6 Adaptive sharpening filter restoration

The images acquired in real time, are usually corrupted by noise and blur. Many denoising filters are proposed in literature [22-23]. The filter has to switch from denoising to edge sharpening according to the local image characteristics. In this method the slope of the edges gets enhanced effectively but the sharpening strength is limited for the other image detail and for texture information. Hence, an adaptive steering kernel regression based sharpening filter algorithm is employed for restoration which takes the local structure of the image into consideration and effectively combines the sharpening and denoising processes. This approach can remove the chrominance artifacts in color images.

3.6.1 Steering kernel construction

The approximation to HR image is obtained by applying the sharpening filter *'S'* on *Y* as

$$\hat{X} = SY = S\,[HX + N_k] \quad ...(26)$$

Since *'S'* is a sharpening matrix used to avoid blur and *Y* is the low resolution image degraded by noise and blur. The

matrix $SH \approx I$ [identity matrix], i.e., S has to invert H globally. But unfortunately the second term SN_k, amplifies the noise as N_k is a high frequency component. One of the possible ways to avoid noise magnificently is to design a sharpening filter adaptive to the local image statistics. In other words, there is no need of inverting H globally. Instead of that the action should be locally controlled to respond to the signal characteristics of the measured image. If there are flat areas of the image where the effect of the blur is not felt, there the sharpening filter should only concentrate on noise reduction and if any region contains an edge, the filter should sharp the image only in the edge direction. Although, many adaptive denoising filters are available [24], filters applying a steering kernel *(sk)* are robust to noise and other degradations. The steering kernel obtains the local structure of images by analyzing the estimated gradients and uses this information to determine the shape and size of the canonical kernel [15].

Assume that the pixel of interest is at $x_i = [x_i, y_i]$, the steering kernel is represented as

$$sk(x_l - x_i) = \sqrt{|c_l|}\exp\{-(x_l - x_i)^T c_l (x_l - x_i)\} \quad ...(27)$$

Where x_i is the center of the steering kernel window, x_l is the given location inside the window and C_l is the covariance matrix estimated in the analysis window from its gradients.

From Eq.(5.4) it is clear that the steering kernel is a simple Gaussian function. However, all the resulting kernel values will not have elliptical contours as the covariance matrix will change at each pixel location. Hence a richer set of shapes can be obtained for the resulting weights. Normally for a flat region in the image, the steering kernel will be flat and isotropic. It basically indicates that the area does not contain any directional structure. If there are any edges in the selected window, the steering kernel will describe the edge out line and the resulting values indicate the similarity of pixel intensity with respect to the pixel in interest. The steering kernel shrinks to smaller regions if the image region contains small scale image details. Even for high level of noise the steering kernel is robust. To compute the steering kernel (*sk*), the procedure for finding covariance matrix should be clear.

The gradient matrix of the window *'W_l'* at the pixel center x_l is described as

$$D = \begin{bmatrix} \cdot & \cdot \\ \cdot & \cdot \\ G_x(x_m) & G_y(y_m) \end{bmatrix} \quad ...(28)$$

Here D is described as the image gradient at position $[x_m, y_m]$. The gradient matrix *'D'* is decomposed using SVD to estimate dominant direction v_1 and its perpendicular direction v_2 in the window W_l.

$$D = U A V^T = U \begin{bmatrix} s_1 & 0 \\ 0 & s_2 \end{bmatrix} \begin{bmatrix} v_1 & v_2 \end{bmatrix}^T \quad ...(29)$$

Where s_1 and s_2 are singular values and they represents the energy in v_1 and v_2 directions respectively.

The covariance matrix C_l of the window W_l is estimated as

$$C_l = \alpha \sum_{i=1}^{2} \rho_i v_i v_i^T \quad ...(30)$$

Here C_l can be written as

$$C_l = \alpha(\rho_1 v_1 v_1^T + \rho_2 v_2 v_2^T)$$

Where $\rho_1 = \frac{s_1 + \xi'}{s_2 + \xi''}$, $\rho_2 = \frac{1}{\rho_1}$ and $\alpha = \left(\frac{s_1 s_2 + \xi''}{M}\right)^k$ …(31)

α and ρ_1 are the elongation and scaling parameters respectively. ξ' and ξ'' are the regularization parameters that reduce the effect of noise and prevent α and ρ_1 from becoming zero. M is the number of samples in the window W_l. α is the structure sensitivity which controls how strongly the local structure can affect the kernel foot prints. Normally the value of α lies in between 0 and 1.5 i.e., $0 \leq \alpha \leq 1.5$. The moderate value of α is 0.1 and if the noise is severe then the α value will also be large.

The sharpening kernel 'S' is given by

$$S = Sk + YL * Sk \quad ...(32)$$

Where S_k is steering kernel, L is the Laplacian operator, * denotes the convolution operator and Y represents the degree of sharpening depending on the local structure of the image. The restored image can then be computed by using weighted average formula (local regression) as follows

$$\hat{f}(x_i) = \frac{\sum_{x \in wl} Sk(x - x_i) y(x)}{\sum_{x \in wl} Sk(x - x_i)} \quad ...(33)$$

Where $y(x)$ is the noisy and blurred image window located at x_l.

If an edge pixel is considered at this instant, due to the negative values on both sides of the edge outline, the sharpening process will be in a direction perpendicular to the edge orientation and if there are positive values along the edge outline, then the kernel smooths the edge. But when it is the case of a flat region, the kernel is viewed mostly as a smoothing filter even though some negative values exist across the region. In practice due to the limited depth of field of cameras, there is a variation of blur component. Due to this, a global sharpening filter will over sharp the regions that are already in focus, resulting in ringing artifacts or overshoots. This may happen with the adaptive approach, if a high value of Y is fixed. To avoid this, the sharpening parameter Y must be adaptive to the local image content sharpness. An image sharpness metric based on singular values are already calculated during the construction of steering kernel. Hence the local metric Q for the pixel located at X_l is defined as

$$Q = s_1 \frac{s_1 - s_2}{s_1 + s_2} \quad ...(34)$$

If the image has more blur, then the Q value will be very low. To avoid overshoots at the edge pixels in the local structure of the image, the parameter Q is taken as a function of sharpness metric γ as

$$\gamma = \begin{cases} \beta & if \quad Q < T_1 \\ \beta(Q - T_2)/(T_1 - T_2) & if \; T_2 < Q < T_1 \\ 0 & if \quad Q \geq T_2 \end{cases} \quad ...(35)$$

Then the sharpening process can be depicted in vector form as

$$\hat{f} = D_{sk}^{-1} S y = D_{sk}^{-1}(Sk + QSkL) y \quad ...(36)$$

Where S is the steering kernel sharpening matrix, steering kernel is (Sk) and D_{sk} is the diagonal matrix of row sums of S which act as normalization factors. $Q = diagonal\ (\gamma_1, \gamma_2 \ldots \gamma_n)$

will assign, sharpening parameters to each pixel. The steering kernel sharpening filter can also be used as chrominance artifact remover while it deals with the colour images.Normally the digital colour images are corrupted by chrominance artifacts and luminance noise. The chrominance artifacts may not be white noise and may contain visually annoying structures for the viewers. Steering kernel can reliably recover the object structures in a grey-scale image. These estimated kernels can be used for both chrominance and luminance channels also. As the human visual system is less sensitive to colour variations, the restored chrominance channels need not be as sharper as the luminance channel. Hence to restore the chrominance channel the sharpening filter can use small constant γ .

The algorithm for color image restoration includes the following steps.

1. The given colour image is converted from RGB to HSI model (Y,C_b,C_r).where Y is the luminance and C_b & C_r are the Hue and saturation which provide the chrominance information.
2. Restore the luminance channel by constructing steering kernels with an adaptive Y according to local blurness.
3. Construct steering kernels for the luminance channel with small Y and restore the yc_b & yc_r.
4. Combine the restored luminance and chrominance channels to estimate the high resolution colour image.

4. RESULTS & DISCUSSION

Two data sets are applied to eliminate the mixed noise in case of low, medium and high density noise conditions. Fig. 6,7 &8 are the low resolution data set-1 at 10% (low), 20% (Medium) and 40% (High) of impulse noise density. Here the additive Gaussian noise with zero mean and variance of 0.02 is considered along with different impulse noise densities. The restored image is shown in the Fig.9(a), (b) &(c). Fig 10,11 &12 are the low resolution data set-2 at low, medium and High density of impulse noise. The restored image is shown in the Fig.13(a), (b) & (c). The reconstructed HR image quality is measured by using quality metrics like Peak signal to Noise Ratio (PSNR), Correlation Coefficient (C.C), Universal Image Quality Index (UIQI), Mean, Standard Deviation (S.D), Entropy and Structural Similarity Index Measure (SSIM). Table.2.provides all these quality metrics for the reconstructed image when compared to the restored output with no noise input. From the results, it is clear that the proposed algorithm provides almost similar results, approximately equal to the output of no noise input at all the noise densities of the mixed noise.

Fig. 6: LR Dataset-I with Low density mixed noise

Fig. 7: LR Dataset-I with medium density mixed noise

Fig. 8: LR Dataset-I with High density mixed noise

(a) (b)

Fig.9 (a)SR output Image for low density mixed noise of Dataset-1
(b) :SR output Image in case of medium density mixed noise for Dataset-1

Fig.9 (c): SR output Image in case of high density mixed noise for Dataset-1

Fig. 10: LR Dataset-2 with Low density impulse noise

Fig. 11: LR Dataset-2 with medium density impulse noise

Fig. 12: LR Dataset-2 with High density impulse noise

(a) (b) (c)

Fig.13 SR output Image of Dataset-2 in case of

(a) low (b) medium (c) high density mixed noise

Table.2. Quality metrics of the reconstructed image in case of Mixed noisy inputs

Quality Metric	SR output image Considering Mixed (Gaussian+ Impulsive) Noise							
	Low input Noise (0.02+0.1)		Medium input Noise (0.02+0.2)		High input Noise (0.02+0.4)		No Noise input	
	Data set1	Data set2	Data set1	Data set2	Data set1	Data set2	Data set1	Data set2
PSNR	40.527	45.597	42.088	45.044	41.738	43.838	46.866	47.694
C.C.	0.827	0.9314	0.8094	0.8776	0.778	0.8464	0.8487	0.8622
UIQI	0.821	0.9314	0.8017	0.8775	0.7636	0.8453	0.8526	0.8617
Mean	118.49	125.58	118.10	129.03	117.50	131.16	118.865	120.077
Entropy	7.1885	6.210	7.2556	6.641	7.3009	6.812	7.2123	6.7072
S.D.	46.336	54.66	47.503	50.033	44.926	46.669	46.669	47.0181
SSIM	0.7329	0.6267	0.5996	0.5954	0.5313	0.5623	0.7861	0.5782

5. CONCLUSIONS

A hybrid algorithm using AGFF technique and Adaptive sharpening filter based SR is proposed to handle the Low resolution images corrupted by mixed noise. From the results it is found that the proposed algorithm reconstructs the image with the similar quality metrics as that of the restored image in case of no noise input LR images and thus can be utilized in the surveillance and forensic applications.

6. REFERENCES

[1] Sung Cheol Park, Min Kyu Park, Moon Gi Kang, May 2003 "Super Resolution Image Reconstruction: A Technical Overview", IEEE Signal processing magazine, Vol 20. No.3 pp: 21-36,

[2] Subhasis Chaudhuri," 2001,Super Resolution Imaging", Kluwer Academic publishers,.

[3] Tania Stathaki, "Image Fusion: Algorithms and Applications" First edition ,Academic Press is an imprint of Elsevier,

[4] Ajay Kumar Nain, Surbhi Singhania, Shailender Gupta and Bharat Bhushan, 2014, " A Comparative Study of Mixed Noise Removal Techniques", International Journal of Signal Processing, Image Processing and Pattern Recognition Vol.7, No.1, pp.405-414

[5] A.Geetha Devi, T.Madhu, K.Lal Kishore, 2015, "Detection, Tracking and Identification of Moving Objects in a Video using Super Resolution - A Novel Approach", International Journal of Applied Engineering Research, ISSN 0973-4562 Volume 10, Number 3, pp. 5471-5487

[6] H. Ur and D. Gross, Mar.1992., "Improved resolution from sub-pixel shifted pictures,"*CVGIP: Graphical Models and Image Processing*, vol. 54, pp. 181-186,

[7] RC. Gonzalez, RE. Woods, 2002."Digital Image Processing",2nd ed., Prentice Hall,

[8] Linwei Yue, Huanfeng Shen, Qiangqiang Yuan, Liangpei Zhang, 2014, "A locally adaptive L1_L2 norm for multi-frame super-resolution of images with mixed noise and outliers", Signal Processing Vol.105, pp:156–174.

[9] Zhengya Xu, Hong Ren Wu, Bin Qiu, and Xinghuo Yu August 2009"Geometric Features-Based Filtering for Suppression of Impulse Noise in Color Images" IEEE transactions on image processing, Vol.18, No.8.

[10] Lowe,D.G., July 2004, "Distinctive Image Features from Scale-Invariant Keypoint", International Journal of Computer Vision,. Vol.59(3), PP:207–232,

[11] Arun K.S., Sarath K.S., October 2010, **"**An Automatic Feature Based Registration Algorithm For Medical Images"**,** International Conference on Advances in Recent Technologies in Communication and Computing., PP:174-177.

[12] David G. Lowe, September 1999, **"**Object recognition from local scale-invariant features**,"** International Conference on Computer Vision, Corfu, Greece, pp. 1150-1157.

[13] Haidawati Nasir, Vladimir Stankovic and Stephen Marshall, 2012, "Singular value decomposition based fusion for super-resolution image reconstruction", Signal Processing: Image Communication 27, pp:180–191.

[14] R. Keys, Dec. 1981 "Cubic convolution interpolation for digital image processing,"IEEE Trans. Acoust., Speech, Signal Process., vol. ASSP-29, no. 6,pp. 1153–1160.

[15] H. Takeda, S. Farsiu, and P. Milanfar, February 2007, "Kernel regression for image processing and reconstruction", IEEE Transactions on Image Processing, 16(2), pp:349–366

[16] Y. Deng, C. Kenney, M. S. Moore and B. S. Manjunath, "Peer group filtering and perceptual color image quantization", vol. 4, July 1999, pp. 21-24

[17] R. H. Chan, C. Ho, and M. Nikolova, Oct. 2005, "Salt-and-pepper noise removal by median-type noise detectors and detail-preserving regularization," IEEE Trans. Image Process., vol. 14, no. 10, pp. 1479–1485.

[18] Y. Shen and K. E. Barner, May-June, 2004, "Fuzzy Vector Median-Based Surface Smoothing", IEEE transactions on visualization and computer graphics, vol. 10, no. 3,

[19] J. Astola, P. Haavisto and Y. Neuvo, April, 1990 "Vector Median Filters", Proceedings of IEEE, vol. 78, no. 4.

[20] E. Abreu, M. Lightstone, S.K. Mitra, K.Arakawa, 1996,A new Efficient approach for the Removal of Impulse Noise from Highly Corrupted Images, IEEE Trans. on Image Processing, Vol. 5, No. 6, pp. 1012-1025.

[21] Vivek Bannore, 2009 "Iterative-Interpolation Super-Resolution Image Reconstruction - A Computationally Efficient Technique", Springer-Verlag Berlin Heidelberg.

[22] A.K.Jain, 1989, "Fundamentals of Digital Image Processing", Engelwood Cliff, N. J.: Prentice Hall.

[23] B. Zhang and J. P. Allebach, May 2008, "Adaptive bilateral filter for sharpness enhancement and noise removal", IEEE Trans. on Image Processing, 17(5):664–678

[24] Syed Ali, "Adaptive Filtering Techniques", IEEE Press, Wiley Inter Science, A John Wiley & Sons, Inc.,Publication